

## Wear Analysis of the Bryan Cervical Disc Prosthesis

Paul A. Anderson, MD,\* Jeffrey P. Rouleau, PhD,† Vincent E. Bryan, MD,‡ and  
Cathy S. Carlson, DVM, PhD§

**Study Design.** *In vitro* wear testing of the Bryan® Cervical Disc prosthesis was performed in a cervical spine simulator. The biologic response was assessed in chimpanzee and goat animal models.

**Objective.** Determine the wear characteristics of the Bryan disc.

**Summary of Background Data.** Large joint arthroplasties fail most commonly by wear and consequent formation of particulate material, which induces an inflammatory response. Therefore, measuring the wear characteristics of the new spinal disc replacements is important.

**Methods.** Six prosthetic assemblies were tested to 10 or 40 million cycles by load and motion and 3 additional assemblies were tested by load only in a cervical spine simulator. Any debris was examined using ASTM standards. The local biologic response to the prosthesis was examined in two chimpanzees. Nine goats were used to assess the biologic response in both local and distant tissues. Arthrodesis was performed on three additional control goats that received an allograft and an anterior cervical plate.

**Results.** Wear results: cervical spine simulators that applied the loads and motions associated with activities of daily living produced wear particulate at a rate of 1.2 mg per million cycles. Device height decreased 0.02 mm per million cycles with approximately 77% of this decrease due to gradual creep of the nucleus under the constant compressive load. Particles generated were granular in shape with a mean feret diameter of 3.9  $\mu\text{m}$ . All animals tolerated placement of the Bryan disc. Wear debris was present in the periprosthetic and epidural spaces in some animals. However, no significant inflammatory response was observed. No wear material was found distant from the implant in draining lymph tissue, the liver, or the spleen.

**Conclusions.** The Bryan disc has satisfactory wear characteristics and does not produce a significant inflammatory response. [Key words: arthroplasty, cervical

spine, Bryan cervical disc prosthesis, prosthetic wear, biologic response, treatment of cervical spine] **Spine 2003; 28:S186–S194**

Cervical disc replacement is a new technology indicated for reconstruction following anterior cervical discectomy in patients having cervical radiculopathy and myelopathy. Its theoretical advantages are to maintain motion, thereby decreasing adjacent segment degeneration, to avoid complications related to fusion, and to allow earlier return to function. Several cervical prostheses have been reported. Pointillart designed a titanium prosthesis that allowed motion between a carbon-bearing surface and the endplate of the superior vertebrae.<sup>1</sup> Unfortunately, 8 of 10 patients had spontaneous fusion within 2 years. The Frenchay disc has two 316 L stainless steel components with a single bearing surface. Each component is fixed to the vertebrae with a screw. At 2 years' follow-up, all 15 patients studied had a high degree of satisfaction and had prosthetic motion averaging 6.5°.<sup>2</sup>

The Bryan cervical disc prosthesis is composed of two clamshell-shaped, titanium endplates that articulate over a load-bearing polyurethane-based polymeric nucleus. There are two bearing surfaces, one each between the polymeric nucleus and each metallic endplate. The prosthesis is unconstrained throughout the normal range of motion and allows coupled motions of angulation and translation. The articulating portion of the device is encapsulated by a sealed, flexible, polymeric sheath that contains a saline lubricant and separates the internal environment from the external *in vivo* environment. The sheath functions as a barrier, preventing soft tissue impingement on the articulating components, and may act as a scaffold for creation of a pseudocapsule over time. The internal articular geometry of the prosthesis is axially symmetric; therefore, flexion–extension motions are representative of both flexion–extension and lateral bending motions.

A pivotal prospective multicenter study of the Bryan Disc was performed in 60 patients.<sup>3</sup> Clinical success at 6 months and at 1 year was 86% and 90%, respectively. No mechanical failures were noted, and no subsidence was encountered. The average range of motion was 9° with a range between 1° and 21°.

Synovial joint arthroplasty failures are largely related to wear of the polymer-bearing surfaces. Wear is associated with mechanical failure of the joint, but more problematic is the inflammatory reaction induced by debris particles. This reaction can result in production of vari-

From the \*University of Wisconsin, Department of Orthopedic Surgery and Rehabilitation, University of Wisconsin Hospitals, Madison, Wisconsin, †Medtronic Sofamor Danek, Memphis, Tennessee, ‡Mercer Island, Washington, §College of Veterinary Medicine, University of Minnesota, St. Paul, Minnesota.

The device(s)/drug(s) that is/are the subject of this manuscript is/are being evaluated as part of an ongoing FDA-approved investigational protocol (IDE) or corresponding national protocol for implantation following cervical discectomy for treatment of radiculopathy and myelopathy.

Benefits in some form have been or will be received from a commercial party related directly or indirectly to the subject of the manuscript. One or more of the author(s) has/have received or will receive benefits for personal or professional use from a commercial party related directly or indirectly to the subject of this manuscript, e.g., honoraria, gifts, consultancies, royalties, stocks, stock options, or decision-making position.

Address correspondence to Paul A. Anderson, MD, University of Wisconsin, Department of Orthopedic Surgery and Rehabilitation, University of Wisconsin Hospitals, 600 Highland Avenue K4/735, Madison WI 53792, USA; E-mail: anderson@surgey.wisc.edu

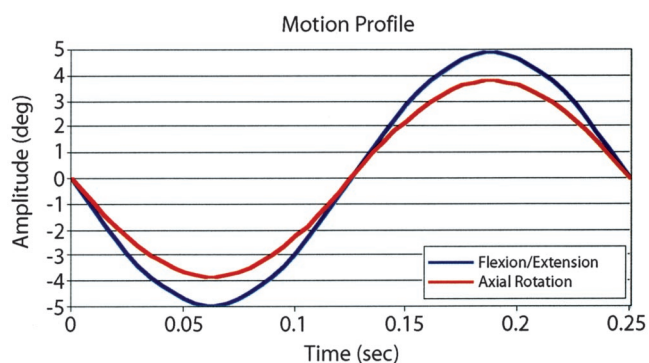


Figure 1. Flexion–extension and axial loading profiles for *in vitro* testing.

ous cytokines that causes bony resorption, a process termed aseptic loosening, loss of bone stock, and ultimately failure.<sup>4,5</sup> Similar failure modes might be expected to occur in spinal arthroplasties. In the spinal column, the presence of inflammatory material in and around the neural elements or neck soft tissues could be catastrophic.

The purpose of this study is to determine the *in vitro* wear properties of the Bryan cervical disc in a cervical spine simulator and to measure the *in vivo* biologic response in two animal models.

## ■ Methods

***In Vivo* Wear Testing.** The test assembly was composed of two simulated endplates, each with an articulating surface identical in material, manufacturing processing, and geometry to the shells used in the implanted device. The polymeric nuclei was placed between the articulating surfaces and encapsulated by the sheath. The assemblies were tested on a cervical spine simulator for 10 million cycles, approximately a 10-year equivalency, in a simulated *in vivo* environment consisting of bovine serum at body temperature.

All nuclei were fully hydrated in a room temperature saline lubricant for at least 72 hours before testing. Tests were performed at body temperature ( $37 \pm 3$  C) in bovine calf serum under the following load and motion profile: 130 N constant load,  $\pm 4.9^\circ$  flexion–extension at 4 Hz, and  $\pm 3.8^\circ$  axial rotation at 4 Hz. One period of the angle profile, for both flexion–extension and axial rotation, is represented in Figure 1.

Following pretest characterization of nucleus height, mass, and diameter, six assemblies were tested by applying both load and motion for 10 million cycles. Three additional assemblies were tested as load-soak controls, subjected only to load. These load-soak assemblies allowed for determination of the fluid absorption and creep effects on the mass and height of the nucleus, respectively. The load-soak assemblies were subjected to load for the same duration of the 10 million-cycle test.

All of the load-bearing polymeric components for the test and load-soak assemblies were weighed and their heights measured before and after testing. On completion of 10 million cycles, all assemblies were visually inspected at 10-power magnification for external signs of damage during manipulation. Three of the test assemblies were tested for sheath integrity by applying 1 Atm internal gauge pressure while submerged.

Two samples were disassembled in order to characterize the

wear particles. The collected particles were placed in deionized water, and the solution was homogenized by manual shaking before sampling. They were evaluated according to ASTM F 1877–98 for feret (maximum) diameter, equivalent circle diameter, elongation, aspect ratio, roundness, and form factor.<sup>6</sup>

An additional four assemblies and two load/soak assemblies were tested until wear of the prosthetic nucleus was sufficient to allow shell-to-shell contact. Identical test conditions were used with the exception that the assemblies did not contain a sheath and were tested in chamber of saline rather than a saline-filled device in a bovine serum bath. This test medium selection is justified by the fact that the device is filled with saline intraoperatively. Absence of the sheath made it possible to assess height, diameter, and mass changes at regular intervals.

**Primate Model.** Twelve adult male chimpanzees had single-level discectomy and reconstruction with the Bryan total cervical disc using standard operative techniques. All animals survived and subsequently had prosthetic removal and allograft interbody fusions. Two animals were assessed for feasibility and eight had implantation of earlier designs of the Bryan disc. Two animals had placement of the currently utilized prosthesis and will be the subject of this analysis. Three months following placement, the animals had prosthesis removal and biopsy of periprosthetic tissues. Tissues were obtained anteriorly adjacent to the prosthesis and from tissues attached to each shell after removal. All tissue samples were marked and fixed with neutral buffered formalin (NBF). The study protocol was approved by the animal care committee.

After decalcification, when appropriate, the samples were embedded in paraffin and sectioned 3 to 4  $\mu$ m thick. Serial sections were stained with hematoxylin and eosin (H&E) and periodic acid-Schiff (PAS). Periodic acid-Schiff–stained sections were used to aid in evaluation of debris particles.

The interior containing the prosthetic disc was lavaged with phosphate buffered saline and the wash was collected. The samples were spun down at 2000 RPM for 20 minutes. The resulting pellet was used to prepare a smear.

The stained sections were evaluated blind by light microscopy to determine the cellular response within the soft and hard tissue surrounding the implants. Samples were also evaluated for the presence of particulate debris. Metal debris was identified by characteristic black particles within the tissues. Polymer particles were identified by their characteristic light birefringence and tendency to stain positive with the PAS stain.

**Caprine Model.** Fifteen skeletally mature female Nubian goats had anterior discectomy at C4–C5 using standard surgical techniques. Ten animals were reconstructed using the Bryan disc (Figure 2). Four animals had reconstruction with iliac crest allograft and an Atlantis (Medtronic, Memphis, TN) plate. One animal was used as a baseline control. Animals were kept caged for 2 weeks and then returned to a large stall with their peers. Animal behavior was recorded and videotaped. The study was performed with approval of the Animal Care Committee.

Animals were grouped as follows:

Group I. Baseline Control, 0-month killing, n = 1

Group II. Bryan™ Cervical Disc prosthesis, 3-month killing, n = 4

Group III. Bryan™ Cervical Disc prosthesis, 6-month killing, n = 3

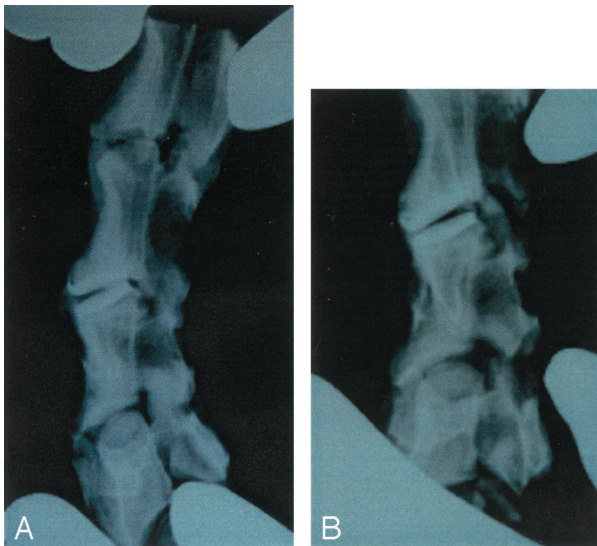


Figure 2. **A**, Flexion radiograph of goat spine taken after sacrifice. **B**, Extension radiograph of goat spine taken after sacrifice.

Group IV. Bryan™ Cervical Disc prosthesis, 12-month killing, n = 3

Group V. Comparative Control (plated), 12-month killing, n = 4

One animal in the plated group sustained a cervical fracture through a screw hole and developed a spinal cord injury. The animal was killed 3 weeks after surgery and was excluded from the study. One animal in Group II died the first postoperative day from gastrointestinal obstruction and was not included in the analysis.

After sacrifice, multiple samples were taken from the following tissues: periprosthetic (anterior, left and right lateral, posterior), draining lymph nodes, liver, spleen, and pinnae of both ears. In addition, laminectomies were performed at C4–C5 and C1–C2 and in the lumbar spine to allow collection of a transverse section of spinal cord at each of these sites.

All of the tissues subjected to histopathological evaluation were fixed in 10% neutral buffered formalin. To ensure that the histologic processing would not dissolve particulates released from the implanted prosthesis, samples of Bryan prosthesis particulates were processed to verify that the PRO-PAR clearant (a xylene substitute) and subsequent processing steps would not damage or dissolve the particulates. The samples were processed in filtered reagents (0.2  $\mu\text{m}$  filter), embedded in paraffin, and sectioned to approximately  $5 \pm 3 \mu\text{m}$  in thickness. All sections were stained using freshly prepared and filtered H & E.

Histopathology evaluations were performed following the ASTM standard for assessing biomaterial compatibility by a board certified veterinary pathologist.<sup>7</sup> Histopathologic assessment of the stained sections included identification of the inflammatory cell types and measurement of the degree of inflammatory reaction. When present, the number of particulates per section was estimated. Evidence of ink migration stemming from the ear tattoo identification markings was also distinguished from any particulates of the implant material by comparison with sections of pinnae from the tattoo sites. The interpretation of the tissue response was based on the histopathological evaluations, which were performed in a blinded manner.

Table 1. Particulate Analysis After 10 Million Cycles

Measure	Min	Max	Average
Feret diameter, $\mu\text{m}$	1.00	454.47	3.89
Equivalent circle diameter, $\mu\text{m}$	0.98	315.26	2.94
Aspect ratio	1.00	8.90	1.38
Elongation	1.00	79.32	1.38
Roundness	0.11	1.00	0.72
Form factor	0.03	1.18	0.74

## Results

### In Vitro Simulation

All test and load-soak assemblies maintained functionality throughout the duration of testing. Examination of the sheaths by 10 $\times$  microscopy revealed no visible cuts, tears, or other signs of wear. For all but one sample, uniform wear was noted on the load-bearing surface of the nucleus. The one exception demonstrated a clustering effect of wear particles in four indentations on the surface of the nucleus and exhibited the highest wear rate of all test assemblies. There was no evidence of metal wear during the particle analysis. Throughout testing, the nucleus successfully prevented the contact of the opposing end plates.

The three test assemblies that were pressure tested to 1 atmosphere gauge pressure to determine sheath integrity all passed the test. Similarly, all test assemblies passed visual inspection for damage to the sheath and disruption to its integrity.

The load-soak control mass change was subtracted from the corresponding test assembly mass change to adjust for fluid absorption under load. The mean, load-soak adjusted, mass loss for the load-bearing nucleus was 1.76%. The load-soak assembly nucleus height represents both the effect of fluid absorption and creep of the material. The average load-soak adjusted height decrease for the test assemblies was 0.75%. Table 1 is a summary of the particle analysis results from the examination of over 2400 independent wear particles. Figure 3 is a histogram of particle size.

Of the four assemblies tested until shell-to-shell contact, one was interrupted due to a problem with the test medium. The remaining three test assemblies were able

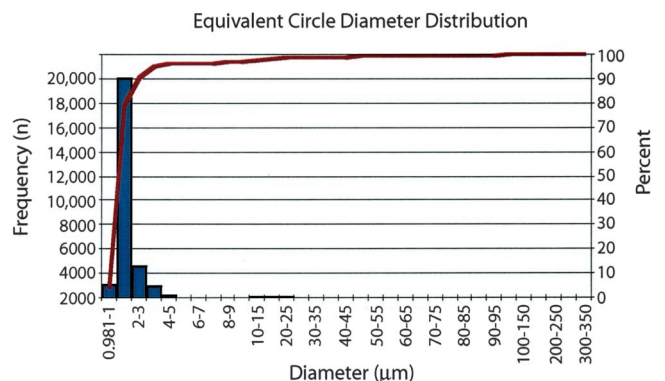


Figure 3. Histogram of particle size.

**Table 2. Histopathologic Results From Periprosthetic and Neural Tissues in Goats**

Group	Animal	Time (mos)	Periprosthetic					
			Fibrous Connective Tissue	Inflammation	Macrophages			Nonmacrophage Polarizable Particulate
					Polarizable Particulate	Nonpolarizable Particulate in Macrophages	Hemosiderin	
I Control	1	0	0	0	0	0	0	0
II 3-month	3	3	+	0	0	0	0	0
	4	3	+	0	0	0	+	0
	5	3	+	0	0	0	0	0
III 6-month	6	6	+	0	0	0	+	+
	7	6	+	0	+	+	0	0
	8	6	+	0	0	+	0	0
IV 12-month	9	12	+	0	0	+	0	+
	10	12	+	0	0	0	+	0
	13	12	+	0	0	+	0	+
V Plated	11	12	+	0	0	++	+	0
	12	12	+	0	0	+++	+	0
	15	12	+	0	0	+++	0	0

to function without kinematic limitations for 37.7, 39.7, and 40 million cycles. The change in prosthesis height as a function of cycle count was linear with a slope of 0.02 mm per million cycles. Shell-to-shell contact did not occur until an average of 18.2% of the nucleus mass was lost due to wear.

### Chimpanzee Results

The two animals recovered unremarkably from both implantation and subsequent prosthesis removal and allograft fusion.

#### Animal 1

**Implant Tissue.** Fibrous tissue and a cellular infiltrate composed primarily of macrophages comprised the tissue adjacent to the implants. A moderate number of polymorphonuclear leukocytes (PMNLs) could also be seen in the tissue adjacent to the caudad shell only. No metal debris or birefringent debris was seen adjacent to either of the shells.

**Periprosthetic.** Anterior soft tissue samples, in general, were composed of fibrous tissue with a mononuclear infiltrate that contained few to large numbers of macrophages. None to a moderate number of neutrophils and few eosinophils were seen in the samples. Some of the samples contained a few to a moderate number of lymphocytes and plasma cells. The majority of the samples contained a few giant cells. No metal particles, few birefringent particles, and only one PAS positive birefringent particle were seen in the samples taken from around the sheath. Little hemosiderin was noted in the majority of the soft tissues.

Lavage samples showed a few metal particles per field, a few birefringent particles, but no PAS positive birefringent particles.

#### Animal 2

**Implant Tissue.** Fibrous tissue and a cellular infiltrate composed primarily of macrophages with a few PMNL comprised the remainder of the tissue adjacent to the implants. A few giant cells were also seen in the tissue adjacent to the caudad shell. No metal debris was seen adjacent to either of the shells. Only one birefringent particle was seen adjacent to the caudad shell.

**Periprosthetic.** Three periprosthetic samples were composed primarily of fibrous tissue. In two of the specimens, a mononuclear infiltrate was present that contained a few macrophages. Two of the samples contained bone fragments. When bone fragments were present, osteoblasts were observed, indicative of bone formation. No osteoclasts were seen. Metal particles were seen in the tissue sample adjacent to the cephalad shell only. There were few particles, and these were seen both intracellularly and extracellularly. Few birefringent particles and no PAS positive birefringent particles were seen. A small amount of hemosiderin was noted in the soft tissue surrounding the cephalad shell only.

Lavage samples showed few metal particles. Few birefringent particles and only one PAS positive birefringent particle

#### Caprine Results

A summary of the histologic results for local, neural, and distant tissue is given in Tables 2 and 3.

#### Group I—Control (Animal #1)

The local tissues were unremarkable. The liver and spleen demonstrated minor abnormalities that were present in many of the experimental and in plated animals. These included hepatic lipidosis (moderate) and splenic hyperemia (severe) and were interpreted to be incidental findings. In addition, several of the lymph

Table 2. Continued

Calcification	Upper		Neural Tissues			Lumbar		
	Polarizable Particulate	NonPolarizable Particulate	Periprosthetic			Calcification	Polarizable Particulate	Nonpolarizable Particulate
			Calcification	Polarizable Particulate	Nonpolarizable Particulate			
0	0	0	0	0	0	0	0	0
0	0	0	0	0	0	0	0	0
0	0	0	0	0	0	0	0	0
0	0	0	0	0	0	0	0	0
0	+	0	0	+	0	0	0	0
0	+	0	+	0	0	+	0	0
0	0	0	+	0	0	+	0	0
0	0	0	0	0	0	0	0	0
0	0	0	0	+	0	0	+	0
0	0	0	+	0	0	+	0	0
0	0	0	0	0	0	0	0	0
0	0	0	0	0	0	0	0	0
0	0	0	0	0	0	0	0	++

node sections contained eosinophilic granulomas, thought to be secondary to parasitism.

#### Group II—Experimental 3-Month (Animals 3, 4, 5)

**Periprosthetic.** None of the periprosthetic sections contained any inflammatory cells or evidence of polarizable particulate material except for one section from Animal #4 that contained low numbers of hemosiderin-laden macrophages. This was interpreted to be secondary to previous hemorrhage in this area and was not considered to be a significant lesion.

**Lymph.** The tissue identified grossly as lymphoid tissue was subsequently identified as thymus.

**Neural.** No abnormalities and no particulate material were identified.

**Distant.** The liver and spleen had nonspecific abnormalities that were unrelated to the prosthetic implantation. No polarizable material was identified.

#### Group III—Experimental 6-Month (Animals 6, 7, 8)

**Periprosthetic Tissue.** Minute to small amounts of polarizable crystalline material were present in all three sections of periprosthetic tissue in one of the animals (Animal #6); however, this material was not associated with any type of tissue reaction, other than hemorrhage in one of the sections (Figure 4). No evidence of this material was present in either of the other animals. Periprosthetic tissue from one of these animals (Animal #7) contained low numbers of macrophages containing pale tan granular material, some of which was weakly polarizable. The appearance of this material was not similar to that of the implant material, however.

**Lymph Tissue.** Lymphoid hyperplasia and granulomatous lymphadenitis were identified in all three animals. This was attributed to the presence of mildly polarizable green, granular, foreign material, which was interpreted to represent tattoo pigment within macrophages (Figure

Table 3. Histopathologic Results From Draining Lymph Nodes, Liver, and Spleen

Group	Animal	Time (mos)	Lymph Nodes						Liver			Spleen	
			Lymphoid Hyperplasia	Green			Granulomatous Lymphadenitis	Eosinophilic Lymphadenitis	Lipidosis	Particulate	Other	Lymphoid Hyperplasia	Hyperemia
				Polarizable Particulate	Polarizable	Nonpolarizable Particulate							
I Control	1	0	++	0	0	0	0	++	++	0	0	+++	
II 3-month	3	3							+	0		+++	
	4	3							0	0	Granuloma	+++	
	5	3							+	0		+++	
III 6-month	6	6	++	0	+	0	++	++	0	0	Mild Cholangitis	++	
	7	6	++	0	0	0	++	++	+	0		++	
	8	6	++	0	++	0	++	0	+	0		++	
IV 12-month	9	12	+	0	++	0	++	+	++	0		0	
	10	12	0	0	+	0	+	+	0	0		++	
	13	12	+	0	+	0	++	0	0	0		0	
V Plated	11	12	+	0	+	0	+	+	+	0		0	
	12	12	++	0	+	0	+	++	+	0		+++	
	15	12	+	0	+	0	+	+	++	0		+++	

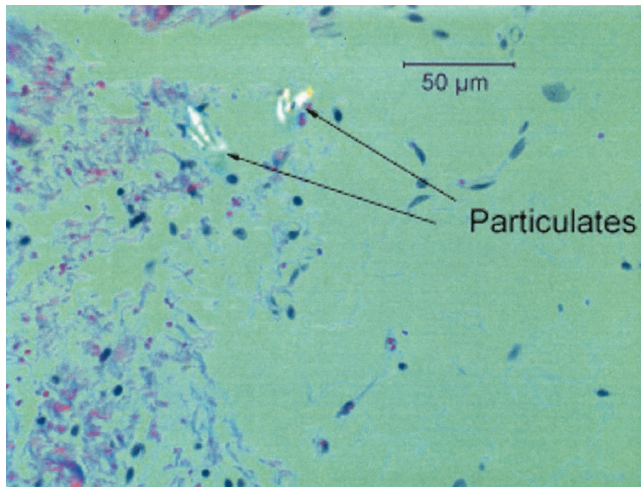


Figure 4. Photomicrograph from goat #6 of periprosthetic tissue showing polarizable debris not associated with any inflammatory response.

5). This material was identical to that present within macrophages in all sections of pinnae, taken from the tattoo sites. No prosthetic polymer or metallic particulate debris was present.

**Neural Tissues.** Sections of spinal cord from one of the animals (Animal #8) contained no significant lesions. Sections from another animal (Animal #6) had minimal amounts of polarizable foreign material, interpreted to be polymer wear debris, in the loose connective tissue exterior to the dura mater in sections of cervical spinal cord but not in the section of lumbar spinal cord. One section of cervical spinal cord from the third animal (Animal #7) contained similar material in the adipose tissue exterior to the dura mater.

**Distant.** The liver and spleen had nonspecific abnormalities that were thought to be unrelated to the pros-

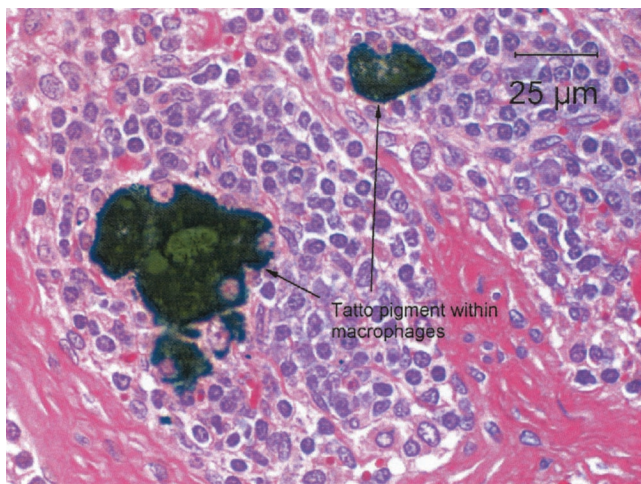


Figure 5. Photomicrograph at high magnification of lymph node section from Animal #7 showing the green/black granular to globular pigment contained in macrophages. H & E stain.

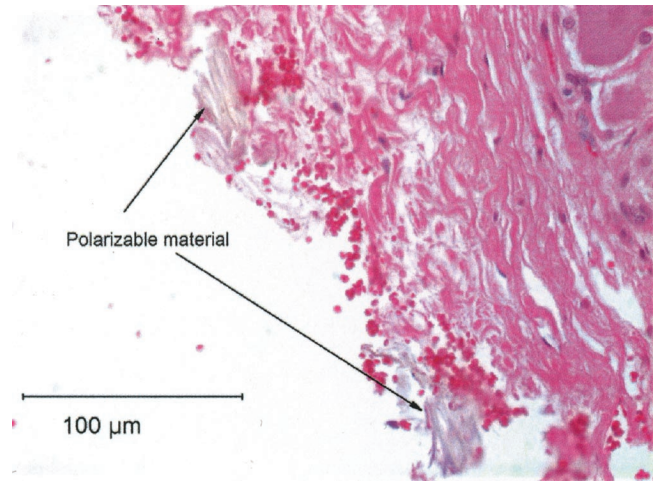


Figure 6. Photomicrograph displays several smaller foci of particulate material in the upper location of the spinal nerve root. H & E stain (original magnification 400 $\times$ ).

thetic implantation. No polarizable material was identified in any of the sections.

#### **Group IV—Experimental 12-Month (Animals 9, 10, and 13)**

**Periprosthetic.** All three sections of periprosthetic tissue from one of the animals (Animal #9) and one of the three sections from another animal (Animal #13) contained multiple small shards of clear, polarizable material, the appearance of which was compatible with debris from the prosthesis. None of these sections contained inflammatory cells centered on the polarizable material; however, 2 out of 3 of the sections from Animal #9 and the section from Animal #13 containing the polarizable material also contained foci of macrophages containing nonpolarizable black granular material. This material was interpreted to represent titanium particles.

Overall, the tissue sections from these 3 12-month animals reveal no lesions to suggest particulate-related disease. The particulates present were extremely small, very low in number, unassociated with any type of tissue response, and located only in connective tissues adjacent to the implant.

**Lymph Nodes.** Similar to the 6-month animals, the lymph tissue had lymphoid hyperplasia and granulomatous lymphadenitis thought to be secondary to tattoo pigments. No polarizable material from the prosthesis was present.

**Neural Tissue.** Two of the sections of spinal cord (one cervical, one lumbar) from one animal (Animal #10) had very small amounts of polarizable particulate material exterior to the dura mater (Figure 6). No inflammatory reaction was present. In the section of lumbar spinal cord, the presumed particulates were present at the extreme margins of the section and were not incorporated into the tissue, suggesting that they may be artifactual.

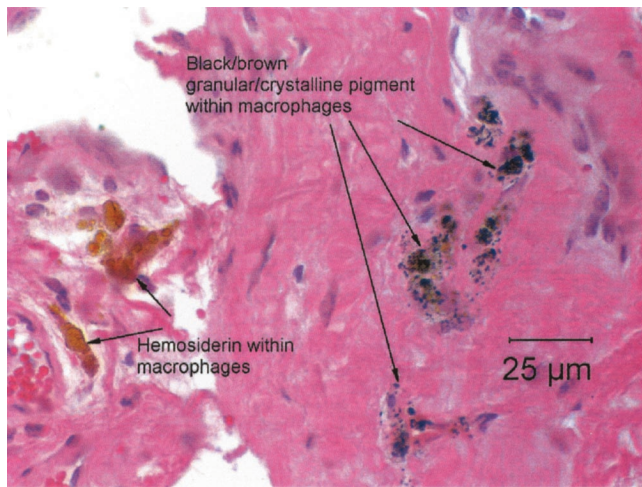


Figure 7. Photomicrograph at high magnification of the left periprosthetic section from Animal #11 showing a small piece of dense fibrous connective tissue containing multiple aggregates of dark black/brown nonpolarizable material that appears to be located within macrophages (right). Compare with hemosiderin (left). H & E stain (original magnification 60 $\times$ ).

**Distant.** The liver and spleen had nonspecific abnormalities that were interpreted to be incidental findings, unrelated to the prosthetic implantation. No polarizable material was identified.

#### Group V—Plated group 12-Month (Animals 11, 12, and 15)

**Periprosthetic.** Macrophages containing dark black/brown nonpolarizable material were identified in sections from all three animals (Figure 7). This pigment most likely represents titanium wear debris from the cervical plate, as it was present in larger quantities than in any of the experimental animals.

**Lymph.** Lymph nodes from all three animals contained a granulomatous lymphadenitis with intralesional green, weakly polarizable pigment that was interpreted to be secondary to the tattooing process. No polarizable material with an appearance similar to debris from the prosthesis was present in any of the lymph nodes. In all three animals, there were foci of eosinophils in the cortex and medulla, sometimes accompanied by plasma cells, some of which were filled with immunoglobulin (Mott cells). The cause of the lymphadenitis in these animals was not identified, but could have been due to a low level of parasitism in these animals.

**Neural Tissues.** Normal. No evidence of particulate debris or inflammation.

**Distant.** The liver and spleen had nonspecific abnormalities were interpreted to be unrelated to the prosthetic implantation. No polarizable or nonpolarizable granular material was identified.

#### Discussion

Standards to test *in vitro* wear have been adopted for hip arthroplasty.<sup>8</sup> The loading patterns, number of cycles,

environment, and many other factors are well described. Use of this standard allows easy comparison among designs and good prediction of clinical performance. Additionally, separate standards have been published to examine wear particulate matter.<sup>6</sup> Although both ASTM and ISO are actively developing intervertebral disc simulator test methods, no similar standards are currently available for disc replacement technology. In testing the Bryan cervical disc, we utilized the principles from these approved and draft standards in the design and operation of the cervical spine simulators.

Normal physiologic motions, or those motions occurring most often during normal daily activities, were assumed to be equivalent to the average neutral zone excursions for the levels indicated for implantation by the Bryan prosthesis (C3–C4 through C6–C7). Flexion–extension and lateral bending have neutral zone excursions of approximately  $\pm 4.9^\circ$ .<sup>9</sup> Axial rotation neutral zones at the same levels in healthy adults measure  $\pm 3.8^\circ$ . An axial compression load of 130 N represents the total joint reaction force at the C7–T1 joint in a neutral position.<sup>10,11</sup> Total joint reaction force is a conservative estimate of disc compression load because the force between adjacent vertebrae is shared between the disc and the two facet joints. These motion and load values were applied continuously at a test frequency of 4 Hz. This frequency is higher than that traditionally used in simulator testing because the shear forces at the articular surface degrade the proteins in the test medium and alter the wear rate. Because the Bryan cervical disc prosthesis has a sealed articular environment that is protein-free, the test rate is limited by local heating and viscoelasticity issues. The steady state temperature rise above that of the test medium at a point 2 mm from the articular surface was measured to be less than 1 Celsius at a test frequency of up to 6 Hz. Likewise, changes in nucleus stiffness due to the inherent viscoelastic properties of the polyurethane were investigated. By measuring nucleus stiffness at a range of frequencies, it was determined that the stiffness change was insignificant over the range from 1 Hz to 4 Hz.

All simulator tests were performed for a minimum of 10 million cycles. It is acknowledged that few data exist that describe how many cervical motion cycles occur per year in healthy, active adults. The neutral zone motions simulated represent over 70% of the total range of motion for the cervical spine in flexion–extension and axial rotation for C0–T1 because the neutral zones of C0–C1 and C1–C2 are very large. Given the magnitude of the applied motions, it is reasonable that 100,000 to 1 million of these cycles would occur per year (11 to 114 cycles per hour), suggesting that a 10 million-cycle simulation represents a minimum of 10 years of clinical use. In comparison, most hip simulator experiments are terminated at 5 million cycles.

The results of the *in vitro* testing demonstrate 1.76% mass loss or a total of 9.6 mm<sup>3</sup> volumetric loss after 10 million cycles. In a separate series of experiments, the

prosthesis was able to withstand up to 40 million cycles before sufficient polymer wear was observed to allow contact between metallic components, which was our definition of failure, although the prosthesis appeared to still function kinematically.

If one assumes that 1 million simulator cycles is representative of a year of clinical use, the rate of wear per year is estimated to be  $0.96 \text{ mm}^3/\text{year}$ . This compares very favorably to wear observed in joint arthroplasty. For example, multiple clinical studies have documented wear rates ranging from 50 to  $100 \text{ mm}^3/\text{year}$  in total hip arthroplasties.<sup>12,13</sup>

The method to examine wear debris was altered from ASTM standards to account for the increased solubility of the polyurethane polymer compared to high-density polyethylene and metals. Similarly, this polymer wear debris proved difficult to isolate in animals to study its biologic effect on neural tissue. Several models have been proposed to assess neurologic biotoxicity such as creation of debris and placement into laminectomy defects or paraspinally. Because of the inability to generate clinically relevant endotoxin-free particles, we chose to study the biologic effect of the entire implant in survival animals. This has the advantage that the debris generated is likely to represent human conditions and that it is localized anterior to the dura and adjacent to the neck soft tissues.

Wear particles, size and shape, varied widely by joint location. Mabrey *et al* analyzed retrieved specimens from revision total shoulder, knee, and hip replacements.<sup>14</sup> Using ASTM standards, they found that the mean equivalent circle diameter was  $0.7 \mu\text{m}$  microns in hips and  $1.2 \mu\text{m}$  microns in shoulders and knees. Other parameters such as roundness, aspect ratio, and elongation factor were different among groups. Animal studies have shown the smaller particles between  $0.24 \mu\text{m}$  and  $4.3 \mu\text{m}$  microns have a more significant inflammatory effect than larger ones. It is hypothesized that different mechanisms of wear are responsible for the variability in particulate size.<sup>15,16</sup>

Prosthetic wear can result in ultimate failure. With loss of bearing surface, the prosthetic can lose function, become stiff, or alternatively unstable. In the spine, this could have significant consequences. No such failures have been observed in the *in vitro* testing, the animal studies, or clinical human studies.

More problematic is the biologic response of tissues to wear debris. Particulate wear matter can be highly proinflammatory, leading to production of various cytokines that activate macrophages and osteoclasts.<sup>4,17-19</sup> These events trigger bony resorption, a process termed aseptic loosening, and clinical failure. Many factors, including the amount of wear debris, the particle size and shape, the material, the ability of macrophages to digest the debris, and the host response are important in determining the adverse inflammatory reaction.<sup>17,19-22</sup> Less well examined is the type of joint. Most arthroplasties have been placed in synovial joints, whereas disc replacements are in fibrocartilaginous joints, a site probably much less

likely to be proinflammatory. The consequences of wear adjacent to neural tissues will need careful study, although in the goat model, no inflammation was seen despite the presence of a few wear particles in both the cervical and lumbar epidural space.

The reaction to wear particles is strongly dependent on the material. Polyethylene appears to produce a more significant response compared to polymethylmethacrylate. Similarly, titanium particles induce a dose-response reaction in macrophages, whereas only mild reactions are created on exposure to low concentrations of cobalt chrome particles.<sup>23</sup> The polyurethanes used in the Bryan disc appear to be biologically well tolerated in other studies, which was confirmed in this study. Substantial data are available on the excellent biocompatibility of medical polyurethanes, which have been used for cardiac applications for decades.<sup>24-26</sup> Furthermore, recent advances in polyurethanes have improved resistance to environmental stress cracking and have made it possible to chemically modify the material to improve wear resistance.<sup>27</sup>

The two animal studies were designed to examine the biologic response to the cervical disc arthroplasty. The histologic results in the chimpanzees and goats were similar. Polymeric wear debris was present in one of two chimps and in three of nine experimental animals. Although only two chimpanzees were tested with the current Bryan disc, the results of the chimpanzee model are important. The anatomy, kinematics, and biologic reaction are similar to humans. No inflammation was present in the periprosthetic tissues despite one having polymeric debris. The overall good performance in the primate is reassuring and allowed human studies to proceed.

Polymeric wear particles were seen in the periprosthetic tissues in three of nine goats. In two of these animals, particulate was seen in the epidural space. In both locations, no inflammatory reaction to this debris was noted; in fact, the particles were all located extracellularly and were not phagocytized by macrophages. It is unknown if the particles originated from the sheath or from the nucleus, as both will generate strongly polarizable particles. These particles are in contrast to the non-polarizable granular material observed in macrophages in two of nine animals. This material was observed in far larger amounts in all of the plated animals.

After surgery, the goat proved to be a harsh model. Normal behavior for these Nubian goats is associated with a significant amount of head butting. Some animals were observed to rear on their hind legs and strike downward with their heads onto their peers' crowns. Despite this violence, no mechanical failures of the prosthesis were observed. Unknown to us initially, when lying supine during surgery, the goat's cervical spine is in a relatively flexed position. Therefore, when upright, the goats extend their cervical spines, compressing the posterior aspect of the prosthesis. We believe this accounted for the tears in the enclosing sheath that were observed posteriorly, as well as the increased wear on the rim of the polymer and the sub-

sequent leakage of debris into the periprosthetic and epidural tissues. However, no inflammatory reaction to the debris was observed, and the particles were in small numbers, especially compared to the plated group.

Concerns over distant effects of wear have been raised. Metal ions have been identified in the urine, liver, lymph, and spleen in failed as well as well functioning total joint replacements.<sup>19,21,22</sup> Metal-on-metal devices generate the greatest likelihood of this phenomenon.<sup>28</sup> Similarly, polymers including polymethylmethacrylate and polyethylene particles have been found in distant sites. We obtained tissue samples from local lymph nodes, liver, and spleen and could not detect wear material.<sup>20</sup>

## ■ Conclusion

The Bryan Total Cervical Disc prosthesis was tested for wear in a cervical spine simulator and in two animal models. After 10 million cycles, 0.75% weight loss occurred. Particle size averaged 3.9  $\mu\text{m}$  microns diameter and had a histogram similar to other arthroplasty wear studies.

The prosthetic implant was tolerated in both animal models. Wear debris was observed in periprosthetic tissues in one of two chimpanzees and in four of nine goats. No inflammatory reaction was observed. Polymeric wear was observed in loose connective tissue in the epidural space without any inflammatory response. In one animal, particles migrated to the lumbar spine. A few particles of metal debris were observed in two experimental goats. The plated group had a far greater amount of metallic debris and inflammatory response. Based on these studies, the Bryan disc has acceptable wear characteristics to predict satisfactory long-term performance.

## ■ Key Points

- *In vitro* testing demonstrates a low wear rate of 1.2 mg per million cycles.
- The procedure was well tolerated and functional in two animal models.
- *In vivo* biologic response was satisfactory without significant inflammatory reaction.

## References

1. Pointillart V. Cervical disc prosthesis in humans: first failure. *Spine* 2001;26:E90–E92.
2. Wigfield CC, Gill SS, Nelson RJ, et al. The new Frenchay artificial cervical joint: results from a two-year pilot study. *Spine* 2002;27:2446–52.
3. Goffin J, Casey A, Kehr P, et al. Preliminary clinical experience with the Bryan Cervical Disc Prosthesis. *Neurosurgery* 2002;51:840–5.
4. Goodman SB, Huie P, Song Y, et al. Cellular profile and cytokine production at prosthetic interfaces. Study of tissues retrieved from revised hip and knee replacements. *J Bone Joint Surg Br* 1998;80:531–9.
5. Goodman SB, Knoblich G, O'Connor M, et al. Heterogeneity in cellular and cytokine profiles from multiple samples of tissue surrounding revised hip prostheses. *J Biomed Mater Res* 1996;31:421–8.
6. ASTM F 1877–98 Standard Practice for Characterization of Particles. In: *ASTM Subcommittee F04.16. Medical Devices and Services*. West Conshohocken, PA: American Society for Testing and Materials; 2003:1582.
7. ASTM F981, Standard practice for assessment of compatibility of biomaterials for surgical implants with respect to effect of materials on muscle and bone. West Conshohocken, PA: American Society for Testing and Materials; 2003.
8. ISO 14242–1, Implant for surgery—wear testing of total hip-joint prosthesis. Part 1: Loading and displacement for wear testing machines and corresponding environmental conditions for test. International Organization for Standardization; 2003.
9. White AA, Panjabi M, ed. *Clinical Biomechanics of the Spine*. 2nd ed. Philadelphia, PA: Lippincott; 2003.
10. Snijders CJ, Hoek van Dijke GA, et al. A biomechanical model for the analysis of the cervical spine in static postures. *J Biomech* 1991;24:783–92.
11. Goel VK, Scifert JL, Totribe K. Biomechanics of a cervical spine interbody fusion cage. Presented at: 27th Annual Meeting of the Cervical Spine Research Society; 2003.
12. Llinas A, Sarmiento A, Ebramzadeh E, et al. Mechanism of failure in hips with an uncemented, all polyethylene socket. *Clin Orthop* 1999;362:145–55.
13. Schmalzried TP, Callaghan JJ. Wear in total hip and knee replacements [comment]. *J Bone Joint Surg Am* 1999;81:115–36.
14. Mabrey JD, Afsar-Keshmiri A, McClung GA, et al. Comparison of UHMWPE particles in synovial fluid and tissues from failed THA. *J Biomed Mater Res* 2001;58:196–202.
15. Mabrey JD, Afsar-Keshmiri A, Engh GA, et al. Standardized analysis of UHMWPE wear particles from failed total joint arthroplasties. *J Biomed Mater Res* 2003;56:475–83.
16. Shanbhag AS, Bailey HO, Hwang DS, et al. Quantitative analysis of ultrahigh molecular weight polyethylene (UHMWPE) wear debris associated with total knee replacements. *J Biomed Mater Res* 2000;53:100–10.
17. Goodman SB, Lind M, Song Y, et al. In vitro, in vivo, and tissue retrieval studies on particulate debris. *Clin Orthop* 1998;352:25–34.
18. Campbell PA, Wang M, Amstutz HC, et al. Positive cytokine production in failed metal-on-metal total hip replacements. *Acta Orthop Scand* 2002;73:506–12.
19. Gelb H, Schumacher HR, Cuckler J, et al. In vivo inflammatory response to polymethylmethacrylate particulate debris: effect of size, morphology, and surface area [erratum appears in *J Orthop Res* 1994;12:598]. *J Orthop Res* 1994;12:83–92.
20. Urban RM, Jacobs JJ, Tomlinson MJ, et al. Dissemination of wear particles to the liver, spleen, and abdominal lymph nodes of patients with hip or knee replacement. *J Bone Joint Surg Am* 2000;82:457–76.
21. Brooks RA, Sharpe JR, Wilmhurst JA, et al. The effects of the concentration of high-density polyethylene particles on the bone-implant interface. *J Bone Joint Surg Br* 2000;82:595–600.
22. Allen MJ, Myer BJ, Millett PJ, et al. The effects of particulate cobalt, chromium and cobalt-chromium alloy on human osteoblast-like cells in vitro. *J Bone Joint Surg Br* 1997;79:475–82.
23. Haynes DR, Rogers SD, Hay S, et al. The differences in toxicity and release of bone-resorbing mediators induced by titanium and cobalt-chromium-alloy wear particles. *J Bone Joint Surg Am* 1993;75:825–34.
24. Bernacca GM, Mackay TG, Gulbransen MJ, et al. Polyurethane heart valve durability: effects of leaflet thickness and material. *Int J Artificial Organs* 1997;20:327–31.
25. de Groot JH, de Vrijer R, Pennings AJ, et al. Use of porous polyurethanes for meniscal reconstruction and meniscal prostheses. *Biomaterials* 1996;17:163–73.
26. Mackay TG, Bernacca GM, Fisher AC, et al. In vitro function and durability assessment of a novel polyurethane heart valve prosthesis. *Artificial Organs* 1996;20:1017–25.
27. Tiwari A, Salacinski H, Seifalian AM, et al. New prostheses for use in bypass grafts with special emphasis on polyurethanes. *Cardiovascular Surg* 2002;10:191–7.
28. Milosev L, Antolic V, Minovic A, et al. Extensive metallosis and necrosis in failed prostheses with cemented titanium-alloy stems and ceramic heads. *J Bone Joint Surg Br* 2000;82:352–7.